



Accelerated Stress Testing by Rotating Disk Electrode for Carbon Corrosion in Fuel Cell Catalyst Supports

Adam Riese,^a Dustin Banham,^{b,*} Siyu Ye,^{b,*} and Xueliang Sun^{a,*}

^aDepartment of Mechanical and Materials Engineering, University of Western Ontario, London N6A 5B9, Canada

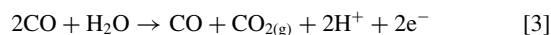
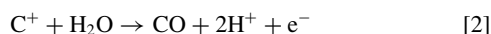
^bBallard Power Systems Inc., Burnaby, BC V5J 5J8, Canada

Durability is one of the key remaining challenges to widespread adoption of proton exchange membrane fuel cells (PEMFCs). The durability and continued high performance of a PEMFC using carbon supported catalysts is highly dependent on the stability of the carbon support. Presently, there are a multitude of accelerated stress test (AST) protocols using rotating disk electrode (RDE) voltammetry to study the corrosion of carbon catalyst support materials, though it remains unclear whether all of these tests provide meaningful reproduction of in-situ membrane electrode assembly (MEA) test results. We evaluate two carbon corrosion ASTs and compare results to MEA data for three well known carbon supported catalysts. Physical characterization of each carbon type by gas sorption, XRD, and Raman, is used to elucidate the observed trends in corrosion resistance and the effects of testing temperature, scan rate, and upper potential limit are examined. We find that AST results are highly dependent on temperature and total testing time, concluding that the first protocol is only valid at 60°C, while the second accurately represents MEA data. This study highlights the importance of different RDE AST parameters when developing ASTs that correlate with in-situ MEA testing. © 2015 The Electrochemical Society. [DOI: 10.1149/2.0911507jes] All rights reserved.

Manuscript submitted February 23, 2015; revised manuscript received April 13, 2015. Published April 30, 2015.

The widespread adoption of proton exchange membrane fuel cells (PEMFCs) for both motive and stationary applications is strongly dependent on reducing costs and improving the durability of the membrane electrode assembly (MEA). Prolonged use can be highly stressful on the MEA, making the loss of performance over the lifetime of the PEMFC one of the key limitations of the technology. Thus the durability of the cathodic catalyst, which facilitates the otherwise sluggish kinetics of the oxygen reduction reaction (ORR), is of particular importance. State of the art PEMFC catalysts use Pt nanoparticles supported by a network of conducting carbon material. These catalyst particles and the supporting carbon must endure harsh operating conditions which include high electrode potentials, acidic environment, and temperatures up to 100°C. Pt catalyst degradation may proceed by several mechanisms including dissolution, Ostwald ripening, and physical agglomeration. The latter two mechanisms are exacerbated by carbon corrosion, which results in a reduction of the overall catalyst surface area.¹⁻³ In addition to this, severe carbon corrosion can lead to physical detachment of the Pt nanoparticle catalysts from the electrode structure, resulting in a total loss of catalytic activity toward the ORR from those detached particles.^{1,4,5}

Carbon corrosion, especially by electrochemical oxidation, has been extensively studied.^{4,6-10} Corrosion may occur by partial oxidation to intermediate surface groups (CO) or via multi-step oxidation to gaseous CO₂. Carbon surface groups may include quinones/hydroquinones, lactones, phenols, carbonyls, and carboxyls.¹¹⁻¹³ One proposed mechanism of oxidation is:^{6,14,15}



While the oxidation of carbon is thermodynamically possible at >0.207 V vs SHE, the kinetics of this reaction are extremely sluggish below 0.9 V. However, in the presence of Pt carbon oxidation may take place as low as 0.6 V.⁸ These conditions, plus high humidity and an acidic environment, make degradation of the support material a point of particular concern. Indeed, carbon corrosion is observed both in real fuel cell systems, especially during start-up and shutdown, and in single cell testing of the MEA. To reach the DOE targeted fuel cell lifetime of 5,000 and 30,000 hours for automotive

and stationary power applications, respectively,¹⁶ it is necessary to use accelerated stress tests (AST) which simulate a long performance lifetime on a timescale that is practical for research and engineering purposes.

Using single fuel cell test stations to test MEAs is a highly effective method for studying the performance of catalysts, catalyst supports, and membranes.¹⁵ MEA testing can be used to demonstrate the activity and durability of a fuel cell in an integrated way because it replicates the variety of operating conditions present in a real-world system. The disadvantage of this method, however, is that it can be difficult to decouple the effects of the myriad parameters and components involved in the system which makes interpreting AST data more complex.

Cyclic voltammetry by thin film rotating disk electrode (RDE) is a convenient alternative for testing fuel cell catalysts and catalyst support materials. Compared to in-situ MEA testing, RDE is advantageous in that catalyst activity can be easily de-convoluted from other components. It requires only small amounts of catalyst material, can often be done within a day, and needs far less of the complicated equipment and infrastructure needed for MEA testing. Though RDE is limited in terms of reproducing the complex environment of a real PEMFC environment, it is highly effective for screening and comparing catalysts and its minimal material requirements make it ideal for research purposes.¹⁷ Currently, there are a wide variety of RDE test protocols employed by different research groups around the world. Due to the nature of RDE testing, variations in test procedures can often lead to vastly different results from one lab to the next.¹⁸ Thus, there is currently a trend to move toward standardization of protocols for catalyst activity and durability to allow more direct comparison of results.¹⁷⁻²¹

Herein we study the effectiveness of RDE AST protocols for evaluating fuel cell catalyst support corrosion. We use three Pt catalysts supported on well-studied carbons: high surface area carbon (HSC), Vulcan carbon (VC), and a highly graphitized, low surface area carbon (LSC). Our test procedures are based on two test protocols suggested by the United States Department of Energy (DOE) for accelerated stress testing of catalyst supports by RDE.²² By using these protocols we hoped to identify trends in carbon corrosion based on changes in electrochemical surface area (ECSA) and mass activity. Our aim is to determine whether these protocols can predict the trends observed during in-situ MEA testing.²³ It is expected that not all RDE ASTs can accurately represent the catalyst support durability observed in real fuel cell systems. In a broader sense, the goal of this study is to highlight the disparities between the data from ASTs done in-situ (MEA) versus those done ex-situ (RDE), and to suggest that a careful selection and evaluation of RDE AST parameters is needed.

*Electrochemical Society Active Member.

²E-mail: siyu.ye@ballard.com; xsun@eng.uwo.ca

Experimental

The carbons used in this work were: high surface area carbon (HSC), Vulcan carbon (VC), and low surface area, graphitized carbon (LSC). HSC and LSC were supplied by TKK and VC was supplied by Cabot. Catalysts used were 47 wt.% Pt/HSC, 50 wt.% Pt/VC, and 47 wt.% Pt/LSC. Catalyst inks were prepared by mixing 3 mg of catalyst, 3 ml of an 80:20 (wt./wt.) mixture of ultra-pure H₂O to isopropyl alcohol, and 30 μ l of 5 wt.% Nafion in alcoholic solution. The mixture was then sonicated to ensure good dispersion and wetting of the catalyst. Two 10 μ l aliquots of ink were deposited onto a polished gold electrode (Pine, AFEST050AUHT, 5.0 mm dia.) and allowed to dry in air. The electrodes were kept stationary during drying. All electrochemical measurements were carried out in 0.09 M H₂SO₄ electrolyte using a Pt wire as the counter electrode and a reversible hydrogen electrode (RHE) as the reference electrode. All potentials reported henceforth are vs. RHE. Each catalyst was activated by cycling from 0.05 to 1.0 at 100 mV/s in N₂ until no changes were observed in the cyclic voltammetry (CV) curve. CVs were recorded scanning from 0.05–1.0 V at 20 mV/s in N₂. ORR activity was measured at 0.9 V on the anodic scan in O₂. ORR and mass activity values are corrected for a baseline scan under N₂. The ECSA was calculated by integrating the area of the CV curve in the hydrogen underpotential deposition (HUPD) region and using the charge value of 210 μ C/cm²_{Pt}, corresponding to a monolayer of adsorbed hydrogen atoms on Pt.

Test protocols were as follows. Protocol A: 5000 cycles, 1.0–1.5 V, scan rate 500 mV/s. This protocol was tested at 25, 40, 50, and 60°C. CVs in N₂ and ORR activity were recorded at 0, 1000, 3000, and 5000 cycles. Protocol B: 6000 cycles, 1.0–1.6 V, scan rate 100 mV/s, tested at 25°C with CVs recorded under N₂ every 1000 cycles and ORR activity recorded at 0, 1000, 2000, and 6000 cycles.

Water vapor sorption analysis was carried out on carbon samples at 40°C using a Quantachrome Hydrosorb-1000. The samples were degassed under vacuum for 18 h at 120°C before analysis. Nitrogen gas sorption data was acquired using a Quantachrome Nova 2000e surface area & pore size analyzer after a degassing at 120°C for minimum 4 hours. X-ray diffraction (XRD) spectroscopy was performed on HSC and VC using a Bruker D8 Advance (Cu-K α source, 40 kV, 40 mA). Raman spectroscopy was performed on HSC and VC using a HORIBA Scientific LabRAM HR Raman spectrometer system with a 532.4 nm laser and optical microscope at room temperature.

Results

The MEA baseline to which we compare RDE results was reported originally by Mukundan et al.²³ MEA testing data was collected using a 50 cm² standard test cell at Ballard Power Systems, Inc. A potential hold at 1.2 V was used to evaluate the durability of three catalysts supported by HSC, VC, and LSC. The carbon catalyst support materials used in the study by Mukundan are the same as those used in this study, albeit with different Pt loadings. We believe that the differences in these carbons are significant enough that clearly distinct trends in durability should be observable despite differences in the Pt loadings. The absolute ECSAs of each catalyst in the present study are given below. Polarization curves were recorded for each after 0, 20, and 400 hours with the exception of HSC which was measured after 100 hours instead of 400 due to a more rapid performance drop. The results of the MEA ASTs are shown in Fig. 1. Each of the catalysts tested shows similar beginning of life (BOL) performance. After a 20 hour potential hold, LSC and VC catalysts remain reasonably stable while HSC catalyst shows a drastic drop in performance. At 100 hours, the performance of HSC has dropped so low as to render a longer potential hold unnecessary. Meanwhile, after 400 hours the performance of the VC drops considerably while LSC shows very little degradation.

The results of the MEA ASTs are not unexpected. The decrease in performance can be correlated to trends in the durability of the carbon support with more stable carbons demonstrating better performance throughout the AST. The apparent durability of the studied catalyst supports, then, is in the order LSC > VC > HSC. These trends in

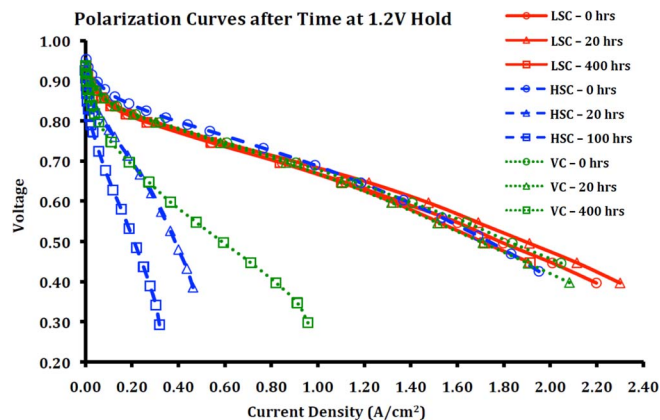


Figure 1. Polarization curves for catalysts supported on LSC, VC, and HSC after different hold times at 1.2 V. Tests were carried out using a 50 cm² fuel cell with serpentine hardware, operated at 80°C in saturated H₂/N₂ at 150 kPa absolute pressure for 400 hours. Reproduced from R. Mukundan, et al.²³

durability are linked to differences in the physical properties of each carbon support, and should be reflected in a well designed RDE AST protocol.

In order to gain insight into the MEA results, we examined physical differences in the three support carbons being studied using several methods. Water vapor and N₂ sorption analysis was performed to determine their sorption properties and surface area while Raman spectroscopy and X-ray diffraction spectroscopy were used to identify differences in their relative degrees of graphitization. Figure 2a shows the N₂ gas sorption isotherm for each of the carbons. The multi-point BET surface areas of HSC, VC, and LSC are 876, 210, and 149 m²/g, respectively. Ignoring, for a moment, the effects of hydrophobicity and crystallinity, the surface area and durability of the carbons are expected to be inversely related. The high surface area in HSC lends itself to rapid degradation as there are many potential oxidation sites. In addition to the kinetic losses associated with carbon corrosion, a further loss in performance may also occur due to increased mass transport resistance arising from the collapse and compaction of the carbon support as it oxidizes to CO₂.²³ This compaction and resulting loss in porosity may be caused by complete oxidation of the carbon to CO₂ which can lead to loss of carbon support material through physical changes to the structure.

The relative hydrophobicity for each of the three carbons was measured using water vapor sorption analysis. A higher affinity for water can improve proton conductivity in real fuel cell systems. However, it also increases the rate of carbon corrosion by oxidation. Increased contact improves water transport which is the source of oxygen for the corrosion reaction.¹⁴ The results of the water vapor sorption analysis are shown in Fig. 2b. In this case the volume of adsorbed water is normalized to each material's specific surface area. This allows for a direct comparison of the hydrophobicity of each carbon material by removing the variance in surface area. The results clearly show that LSC has the lowest volume of adsorbed water, meaning that it is the most hydrophobic of the three carbons. VC and HSC showed similar hydrophobicity but HSC had the highest adsorbed water content, making it most hydrophilic. Thus, the hydrophobicity increases as HSC < VC < LSC, which matches both the trends in surface area (Fig. 2a), and durability (Fig. 1). The hydrophobicity of LSC may be related to its higher degree of graphitization compared to the other two carbons.

XRD and Raman spectroscopy were also done for HSC and VC, and are shown in Fig. 2c and Fig. 2d. As shown in Fig. 2c, the (002) peak and (100) peak are clearly visible for both carbon materials. While the XRD spectra are similar, the (002) peak is broader for the HSC material, which points to less crystallinity compared with VC. Raman spectroscopy is another powerful tool for analyzing carbon samples. The results of Raman analysis on HSC and VC are

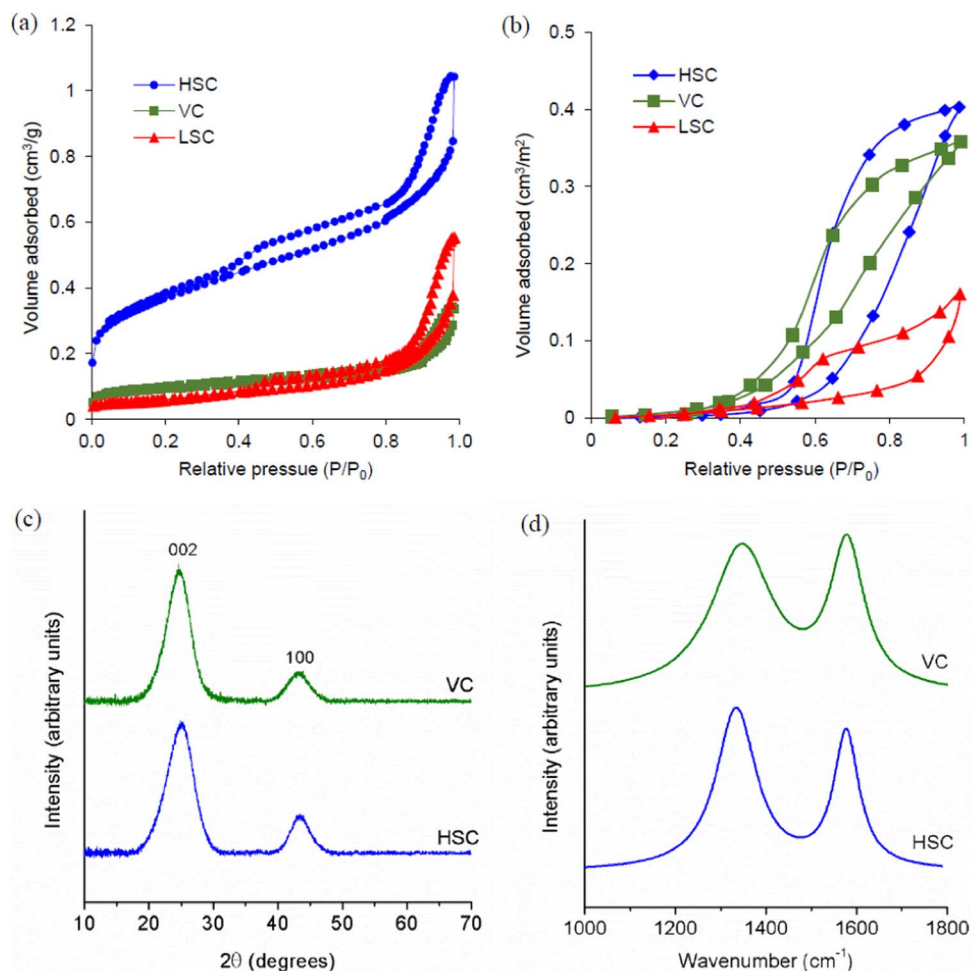


Figure 2. (a) Sorption isotherms of N₂ (a) and H₂O (b) on HSC, VC, and LSC (exclusive of Pt). (c) XRD and (d) Raman spectra of HSC and VC.

shown in Fig. 2d. The most meaningful range of wavenumbers for carbon black is between 1000 and 1800 cm⁻¹ where the D-band and G-band appear.²⁴ For the carbon samples, the D-band occurs around ~1345 cm⁻¹ and corresponds to amorphous carbon while the G-band, which appears at ~1580 cm⁻¹ corresponds to sp² carbon (ie: more graphitic). Others have examined carbon black using Raman spectroscopy and used the ratio of the integrated intensities of the D and G bands, I_D/I_G, as a measure of the level of crystallinity in the sample.²⁴ HSC was measured to have a I_D/I_G value of 1.89, with D- and G-band peaks at 1338 and 1585 cm⁻¹, respectively. VC had an I_D/I_G value of 1.83 and D- and G-bands centered at 1347 and 1578 cm⁻¹, respectively. The higher an I_D/I_G value in HSC indicates a slightly more disordered carbon, although the values are similar.

Taken together, the N₂ and H₂O sorption data (Fig. 2a and 2b), XRD data (Fig. 2c) and Raman data (Fig. 2d) clearly explain the in-situ durability trend observed for the three catalysts (Fig. 1). This is important, as the ultimate goal of this study was to evaluate the ability of RDE ASTs to accurately predict in-situ MEA trends in catalyst durability. Clearly, any reliable RDE AST should demonstrate the following trend in catalyst stability: HSC < VC < LSC.

Many previous studies have used RDE to perform ASTs on carbon supported catalysts for PEMFCs. Some have investigated the effect of potential range on the oxidation of carbon,²⁵ others have used RDE ASTs for potential cycling coupled with CO₂ monitoring or electron microscopy to investigate the support corrosion.^{26,27} Very recently, a protocol comparable to one used in this study has been used to compare HSC with a ceramic catalyst support to highlight the excellent durability of the latter.²⁸ The AST protocols selected for this work were suggested by the US Department of Energy,²² and will

herein be referred to as protocol A and protocol B. Protocol A consists of cycling under N₂ from 1.0–1.5 V vs. RHE at 500 mV/s for 5000 cycles at 60°C. Protocol B consists of cycling under N₂ from 1.0–1.6 V vs. RHE at 100 mV/s for 6000 cycles at 25°C. The former is done at elevated temperature, but with a lower upper potential limit (UPL) of 1.5 V compared to a UPL of 1.6 V in the protocol B. The two protocols are alternatives, with one requiring a single 8-hour working day (protocol A), and one which takes roughly 24 hours to complete (protocol B). The chosen potential range above 1.0 V prevents the reduction of formed Pt oxide, minimizing the effect of Pt dissolution caused by repeated redox reactions, and isolating the effects of carbon corrosion.²⁹ Although others have shown the presence of Pt to enhance carbon oxidation^{8,30} in PEMFCs, the carbon materials in this study are significantly different, as seen in the physical characterization data, to reliably illustrate the different trends seen during in-situ durability studies.

Using protocol A, we first tested the durability of each carbon at 25°C. The CVs obtained for Pt/HSC at 0, 1000, 3000, and 5000 cycles are shown in Fig. 3a. As is clear, there is almost no change in the CV curves before and after the AST at 25°C. The initial ECSA values of Pt/HSC, Pt/VC, and Pt/LSC at 25°C were 75.1, 39.6, and 45.5 m²/g, respectively. These values very closely agree with those reported for the catalysts tested in Fig. 1 (HSC: 74 m²/g, LSC: 44 m²/g, VC: not explicitly stated). The inset in Fig. 3a shows a highlight of the capacitive double layer region from roughly 0.4–0.6 V for the 25°C AST. Even with this expanded view there is very little change seen in the curves, suggesting good support durability. This result is surprising, given that HSC demonstrated rapid performance loss in MEA testing. It is apparent from the results of the AST that, at

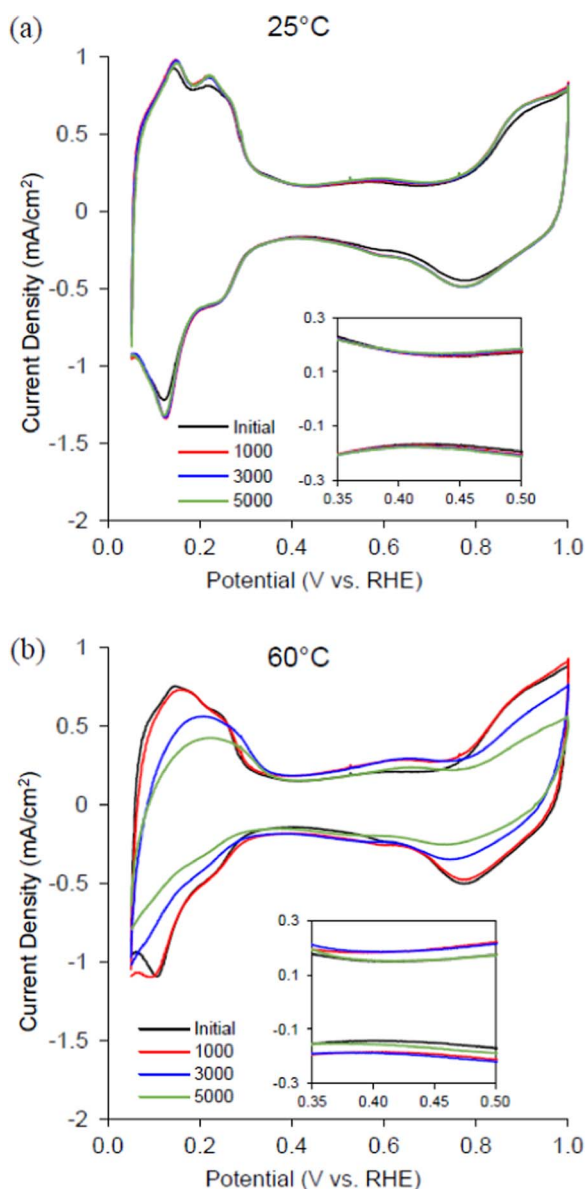


Figure 3. Cyclic voltammograms of HSC catalyst at different cycles for (a) 25°C and (b) 60°C. Cycling at 500 mV/s from 1.0–1.5 V vs. RHE in 0.09 M H₂SO₄.

25°C, this protocol is not aggressive enough to accurately reproduce the results seen in-situ. In order to improve the predictive capabilities of the AST, we repeated protocol A at 60°C; the CV curves from this test are shown in Fig. 3b. There is considerably more degradation of the carbon sample at 60°C than at 25°C, as seen in the change in CV curves with cycling. The HUPD region from roughly 0.05–0.4 V decreases in size with cycling especially for the 60°C AST, pointing to a decreasing ECSA. The inset in Fig. 3b highlights the capacitive double layer region for the 60°C case, showing notable changes in the double layer capacitance. At the elevated temperature, the double layer capacitance increases from 0 to 1000 to 3000 cycles, finally decreasing at 5000 cycles. The increase in the double layer charging current is likely due to both an increase in the pseudo-capacitive groups on the surface of the carbon, as well as an increase in the carbon surface area, which may arise due to the creation of micropores as CO₂ is formed. After 5000 cycles the double layer appears to have reduced, which may indicate the removal of surface species and loss of carbon material. Indeed, it has been previously reported that severe oxidation may result in some surface species being removed, hence lowering

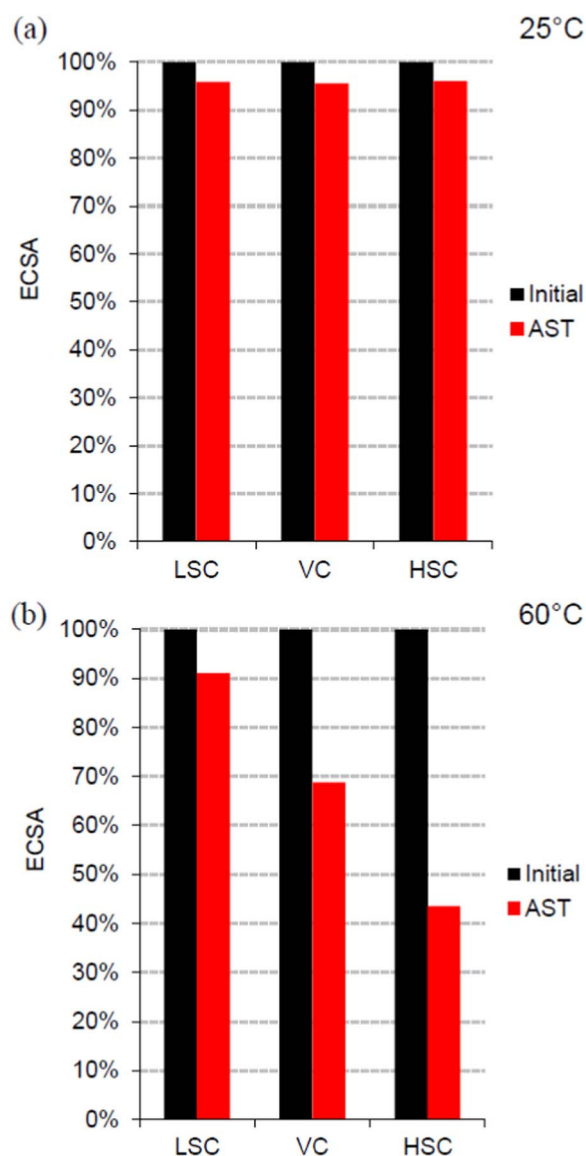


Figure 4. Calculated ECSA at BOL and after 5000 cycles for catalysts on HSC, VC, and LSC at 25°C (a) and 60°C (b). 5000 cycles at 500 mV/s from 1.0–1.5 V vs. RHE in 0.09 M H₂SO₄.

the coulombic charge in the double layer region.⁷ The changes in the double layer region for the 60°C AST reflect the extreme degradation seen in MEA testing for HSC.

Pt/VC and Pt/LSC were also tested using protocol A at 25°C and 60°C, and their ECSA values are plotted, along with those of Pt/HSC, in Fig. 4. For the AST at 25°C, Pt/LSC, Pt/VC, and Pt/HSC each retains 96% of their original ECSA after testing. This result is surprising and clearly not in agreement with MEA data. When the same protocol is carried out at 60°C, the ECSA values drop from their original value to 91%, 61%, and 44% for Pt/LSC, Pt/VC, and Pt/HSC after cycling. This trend of degradation matches much more closely to that seen in the MEA data. These results indicate a strong dependence on testing temperature for AST RDE protocols.

To further examine the influence of temperature on carbon corrosion during ASTs, protocol A was done using Pt/HSC at several temperatures between 25 and 60°C. The results of these tests are shown in Fig. 5. There is a clear trend of decreasing ECSA and mass activity with increasing temperature after the AST. After 5000 cycles the ECSA decreases from initial values to 96%, 79%, 70%, and 44% for tests at 25, 40, 50, and 60°C, respectively. Mass activity shows a

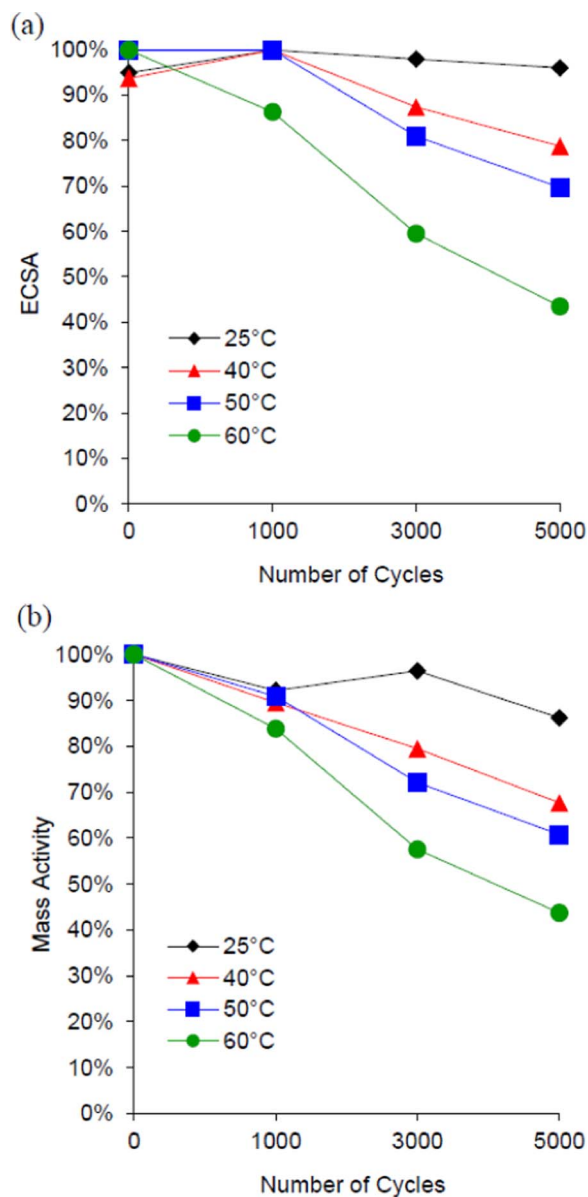


Figure 5. ECSA (a) and mass activity (b) after AST cycling at 25, 40, 50, and 60°C for Pt/HSC. Cycling at 500 mV/s from 1.0–1.5 V vs. RHE in 0.09 M H₂SO₄.

similar trend with post-AST activities of 88%, 68%, 61%, and 44% of initial values for the 25, 40, 50, and 60°C tests, respectively. We have found that, at 25°C, protocol A does not accurately predict the in-situ MEA data. This suggests the need for elevated temperature, or a more aggressive AST protocol when using ambient temperature, in order to accurately represent in-situ PEMFC degradation.

While performing protocol A at 60°C does appear to reliably predict in-situ MEA trends in catalyst stability, it is desirable to have an RDE AST protocol that can be run at room temperature. This is because many RDE electrodes cannot be used at temperatures >25°C. Protocol B uses a lower scan rate of 100 mV/s and is carried out at 25°C, with an UPL of 1.6 V. For Pt/HSC, the ECSA value recorded after 4000 cycles is just 17% of the original, and after the full 6000 cycles, the carbon has degraded so much that calculation of the ECSA from the CV curve is not meaningful. Furthermore, the mass activity for Pt/HSC dropped by 75% after this AST. Meanwhile, for Pt/LSC, reasonably good durability is seen with ECSA values at 4000 and 6000 cycles of 90% and 86% of the original, respectively. Pt/LSC

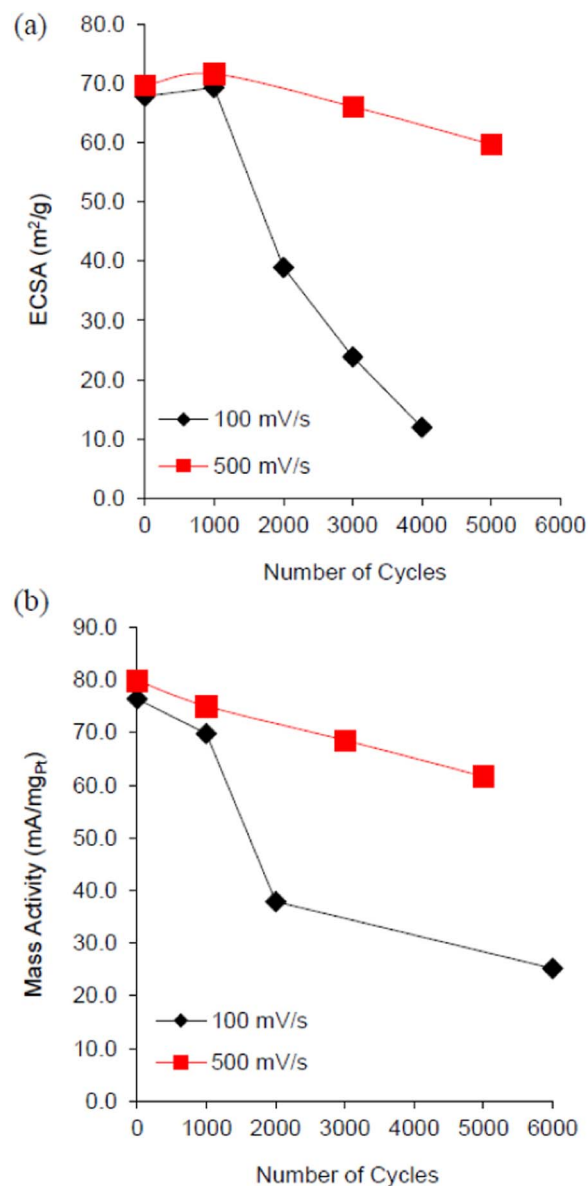


Figure 6. ECSA (a) and mass activity (b) of HSC catalyst at 25°C, cycling from 1.0–1.6 V vs RHE at 100 mV/s and 500 mV/s, respectively.

exhibited a reduction in mass activity of 34% after AST. Importantly, the results of these tests align well with in-situ MEA data for the HSC and LSC supported catalysts.

The two protocols originally suggested have different UPL and different scan rates. Both parameters can affect the outcome of an AST. Figure 6 shows the ECSA (a) and mass activity (b) of Pt/HSC tested at 25°C by a modified protocol A with UPL of 1.6 V, rather than 1.5 V, and protocol B. The modified Protocol A, with scan rate of 500 mV/s and 5000 cycles has a total cycling time of 200 minutes. Protocol B has a scan rate of 100 mV/s and 6000 cycles for a total cycling time of 1200 minutes. It is clear from Fig. 6 that the longer, slower AST is considerably more aggressive on the carbon supported catalysts. For protocol B, the hydrogen adsorption region became almost negligible beyond 4000 cycles so that no ECSA values could be reported. If we examine the ECSAs after the first 200 minutes it appears that the faster scan rate of protocol A is more aggressive. After 200 minutes, the ECSA of Pt/HSC drops to 83%, having cycled 5000 times at 500 mV/s. During the same time in protocol B, having only completed 1000 cycles at 100 mV/s, the ECSA of Pt/HSC remains unchanged. We can say, then, that a faster scan rate and increased

cycle number is more aggressive, if the total test time is kept constant. However, for a given number of cycles, a slower scan rate of 100 mV/s and correspondingly longer time is drastically more aggressive than a high scan rate of 500 mV/s with less total test time. This can be explained by the amount of time spent at high potentials between 1.0–1.6 V where carbon oxidation is favorable. These results imply that time spent holding the catalyst in this potential range is more effective in corroding the carbon support than repeated, rapid cycling. Each of these test protocols was also performed on Pt/LSC with minimal degradation noted. Even with a UPL of 1.6 V, the more accelerated, protocol A at room temperature does not produce the same trend of degradation as seen in the MEA data or in the 60°C test with UPL of 1.5 V.

The importance of temperature, scan rate, and total scanning time has been highlighted. In terms of reproducing the support corrosion data seen in MEA testing, protocol A is appropriate only when used at elevated temperature (60°C) and not at room temperature. Protocol B reproduces the results from the MEA testing well. While the comparison with the MEA data is only qualitative, it is the trend in support degradation that is of importance. This study may be useful for further development of RDE ASTs not only for carbon corrosion but for overall catalyst degradation. When selecting AST parameters, careful consideration should be given to temperature, potential window, scan rate, UPL, and total scanning time. This study highlights the need for efforts toward standardized RDE testing and ensuring that the technique is accurately representing real PEMFC data.

Conclusions

AST protocols designed to study catalyst support corrosion by RDE were evaluated using three representative carbon types which have been well studied in previous literature. The objective of this study is to bring to attention the drastic inconsistencies between MEA (in-situ) and RDE (ex-situ) carbon durability data that may arise if the RDE protocol is not carefully considered. As there are many AST protocols being used by various labs, it is worth highlighting this potential difference as the trends observed from RDE data may not accurately represent the durability of catalyst supports in real fuel cell systems. This is especially important for correctly screening catalyst support materials which are likely much more similar than those studied here. It was determined that for protocol A (5000 cycles from 1.0–1.5 V at 500 mV/s), elevated temperature of 60°C is necessary to reproduce the degradation observed in MEA tests. When performed at 25°C, this particular AST showed no noticeable signs of degradation to an HSC supported catalyst which is otherwise known to have poor durability. Thus, temperature is shown to have a considerable effect on the durability of carbon supports during RDE ASTs. Protocol B (6000 cycles from 1.0–1.6 V at 100 mV/s) results in carbon corrosion data which agrees well with MEA data even when performed at room temperature. Additionally, potential scan rate is also shown to affect support durability protocols insofar as they result in longer exposure to high potentials, which accelerates corrosion. The drastic differences in end of test ECSAs and activities following these ASTs provide further evidence that carbon support durability is critical to overall catalyst durability. Importantly, it is found that not all RDE AST protocols can accurately represent the durability of carbon sup-

ports in fuel cell systems. Hence, a careful selection of parameters is needed to produce meaningful results via the RDE method.

Acknowledgments

This work was supported by Ballard Power Systems Inc., Natural Sciences and Engineering Research Council of Canada (NSERC), the Canada Research Chair (CRC) Program, the Automotive Partnership of Canada through the Catalyst Research for Polymer Electrolyte Fuel Cells (CaRPE-FC) program, and the University of Western Ontario.

References

1. P. J. Ferreira, G. J. la O', Y. Shao-Horn, D. Morgan, R. Makharia, S. Kocha, and H. A. Gasteiger, *J. Electrochem. Soc.*, **152**, A2256 (2005).
2. J. Zhang, Ed., *PEM Fuel Cell Electrocatalysts and Catalyst Layers*, Springer London, London (2008).
3. X. Yu and S. Ye, *J. Power Sources*, **172**, 145 (2007).
4. L. M. Roen, C. H. Paik, and T. D. Jarvi, *Electrochem. Solid-State Lett.*, **7**, A19 (2004).
5. S. Swathirajan and B. Merzougui, in *ECS Transactions*, vol. **2**, p. 21, ECS (2007).
6. J. Thomas, *Carbon N. Y.*, **8**, 413 (1970).
7. K. Kinoshita and J. Bett, *Carbon N. Y.*, **11**, 403 (1973).
8. K. Kinoshita and J. A. S. Bett, *Carbon N. Y.*, **12**, 525 (1974).
9. D. Lowde, J. Williams, and B. McNicol, *Appl. Surf. Sci.*, **1**, 215 (1978).
10. J. Willsau and J. Heitbaum, *J. Electroanal. Chem. Interfacial Electrochem.*, **161**, 93 (1984).
11. H. Boehm, *Carbon N. Y.*, **32**, 759 (1994).
12. F. Rodríguez-reinoso, *Carbon N. Y.*, **36**, 159 (1998).
13. M. Tarasevich, V. A. Bogdanovskaya, and N. M. Zagudaeva, *J. Electroanal. Chem. Interfacial Electrochem.*, **223**, 161 (1987).
14. K. H. Kangasniemi, D. A. Condit, and T. D. Jarvi, *J. Electrochem. Soc.*, **151**, E125 (2004).
15. S. Maass, F. Finsterwalder, G. Frank, R. Hartmann, and C. Merten, *J. Power Sources*, **176**, 444 (2008).
16. M. K. Debe, *Nature*, **486**, 43 (2012).
17. Y. Garsany, J. Ge, J. St-Pierre, R. Rocheleau, and K. E. Swider-Lyons, *J. Electrochem. Soc.*, **161**, F628 (2014).
18. Y. Garsany, J. Ge, J. St-Pierre, R. Rocheleau, and K. Swider-Lyons, *ECS Trans.*, **58**, 3 (2013).
19. Y. Garsany, O. A. Baturina, K. E. Swider-Lyons, and S. S. Kocha, *Anal. Chem.*, **82**, 6321 (2010).
20. S. S. Kocha, *2014 DOE Hydrogen and Fuel Cells Program Review* (2014), http://www.hydrogen.energy.gov/pdfs/review14/fc111_kocha_2014_o.pdf.
21. S. S. Kocha, J. W. Zack, S. M. Alia, K. C. Neyerlin, and B. S. Pivovar, *ECS Trans.*, **50**, 1475 (2013).
22. S. S. Kocha, Y. Garsany, and D. Myers, *DOE Webinar* (2013), <http://energy.gov/eere/fuelcells/downloads/testing-oxygen-reduction-reaction-activity-rotating-disc-electrode>.
23. R. Mukundan, G. James, D. Aytote, J. R. Davey, D. Langlois, D. Spornjak, D. Torraco, S. Balasubramanian, A. Z. Weber, K. L. More, and R. L. Borup, *ECS Trans.*, **50**, 1003 (2013).
24. T. Jawhari, A. Roid, and J. Casado, *Carbon N. Y.*, **33**, 1561 (1995).
25. H.-S. Choo, T. Kinumoto, M. Nose, K. Miyazaki, T. Abe, and Z. Ogumi, *J. Power Sources*, **185**, 740 (2008).
26. H. R. Colón-Mercado, H. Kim, and B. N. Popov, *Electrochem. commun.*, **6**, 795 (2004).
27. F. Xu, M. Wang, Q. Liu, H. Sun, S. Simonson, N. Ogbeifun, E. A. Stach, and J. Xie, *J. Electrochem. Soc.*, **157**, B1138 (2010).
28. J. Parrondo, T. Han, E. Niangar, C. Wang, N. Dale, K. Adjemian, and V. Ramani, *Proc. Natl. Acad. Sci. U. S. A.*, **111**, 45 (2014).
29. J. Wang, G. Yin, Y. Shao, S. Zhang, Z. Wang, and Y. Gao, *J. Power Sources*, **171**, 331 (2007).
30. E. Passalacqua, P. L. Antonucci, M. Vivaldi, A. Patti, V. Antonucci, N. Giordano, and K. Kinoshita, *Electrochim. Acta*, **37**, 2725 (1992).